# Out-of-Band Distortion in Massive MIMO: What to expect under realistic conditions?

Laura Monteyne\*, Gilles Callebaut\*, Björn Sihlbom<sup>†</sup> and Liesbet Van der Perre\*

\*Department of Electrical Engineering, KU Leuven, Belgium

<sup>†</sup>Research Center at Huawei Technologies, Gothenburg, Sweden

E-mail: laura.monteyne@kuleuven.be

*Abstract*—Massive Multiple Input Multiple Output (MIMO) offers superior capacity for future networks. In the quest for energy efficient implementation of these large array-based transmission systems, the power consumption of the Power Amplifiers (PAs) is a main bottleneck. This paper investigates whether it is possible to operate the PAs in their efficient nonlinear region, as the Out-of-Band (OOB) distortion may not get the same array gain as the in-band (IB) signals. We present a framework to simulate the effects under realistic conditions, leveraging on an accurate Ray-Tracing Simulator (RTS). The results show that the often assumed i.i.d. Rayleigh fading channel model results in too optimistic predictions, also in Non Line of Sight (NLoS) multi-path scenarios, regarding the spatial distribution of OOB emissions. We further comment on the consequences in view of current regulatory constraints.

Index Terms—Mobile communication, massive MIMO, lowcomplexity hardware, power amplifiers, nonlinear distortion

#### I. INTRODUCTION

Massive MIMO is a key technology to achieve high spectral efficiency and capacity gain for the 5G network, especially in dense urban environments. The challenge is to build such large systems to process a massive number of antenna signals at reasonable complexity. The need for energy efficiency, low complexity and thus low-cost hardware components is evident. In modern cellular networks, the Base Station (BS) and more specifically its PAs, are the biggest energy consumers [1]. Several studies suggest the possibility of implementing massive MIMO systems with low complexity hardware, while maintaining the high performance [2], [3]. Unfortunately, a reduced complexity in the PA hardware results in higher nonlinearities and thus in IB and OOB distortions [4]. OOB distortions are defined by ITU-R [5] as emissions on a frequency immediately outside the necessary frequency bandwidth and could affect neighbouring applications. The analysis in this paper focuses on OOB distortions, while it is considered that IB performance should be guaranteed at all times.

Several studies on the impact of nonlinear amplification in massive MIMO transmission have been conducted. They are mostly based on relatively simple models for both channels and distortions, such that it is possible to derive closed form analytical expressions. Authors have assumed that distortions due to nonlinear amplification can be considered uncorrelated in i.i.d. Rayleigh fading conditions. Consequently, their impact highly reduces with increasing number of antennas [2]. However, in many cases the uncorrelated terms assumption is not valid and for example, it has been shown that in Line of Sight (LoS) situations with a single or dominant user, the OOB distortion will get an array gain in the direction of the intended user [6]. The directivity of OOB distortions due to nonlinear amplification has been further studied for multiuser scenarios [7], where also Intermodulation (IM) beams [8] are predicted. In the published state-of-the-art, omnidirectional antennas have been typically assumed, which are practically not feasible nor desirable in view of mutual coupling. In summary, the state-of-the-art presents different theoretical results that leave the question open what to expect under realistic conditions. To draw relevant and reliable conclusions, realistic models and assumptions are required.

The main objective of this study is to investigate and analyze the impact of low-power transmitters, based on lowcost hardware, on the OOB distortion in a massive MIMO system under realistic conditions. Do nonlinear PAs in massive MIMO cause correlated IB and OOB distortions and under what circumstances are these distortions problematic with respect to current regulations? We specifically investigate the spatial distribution of OOB distortions in massive MIMO.

The results in this paper are generated by a versatile yet robust simulation framework for the analysis of OOB radiation in a massive MIMO environment under realistic conditions. In particular, channel modeling in the simulation framework is realized with advanced RTS software, provided by Huawei Technologies Sweden. Several evaluation metrics are defined and graphical heatmaps for the spatial distribution of the OOB radiation are presented to quantify and measure the impact of the nonlinear characteristics of the PAs. We study both random scenarios and 'handpicked' use cases that are created to provoke potentially worst case impact in terms of OOB emission. Finally, we analyze and interpret the results.

The second section introduces the simulation framework that is established with the purpose of modeling and analyzing OOB emission in massive MIMO transmission. We define the evaluation metrics that are used to compare and assess different scenarios. In Section III, we describe the set-up for the performed experiments to analyze OOB distortion.

This paper is accepted and published in the Conference Proceedings of 2021 IEEE 94th Vehicular Technology Conference (2021).

The results of this analysis are presented and discussed in Section IV. Section V discusses the current OOB regulations in view of the spatial distribution of OOB occurring from massive MIMO transmission. Finally, the main conclusions are summarized in section VI, along with future work.

#### **II. SIMULATION FRAMEWORK**

A high-level overview of the simulation framework is given in Fig. 1. The first building blocks generate random data and maps it to the 16-Quadrature Amplitude Modulation (QAM) constellation. The symbols are modulated to an Orthogonal Frequency-Division Multiplexing (OFDM) signal based on the LTE-format. Pulse shaping is realized with a root raised cosine filter with a roll-off factor  $\alpha_{RRC} = 0.22$ . Maximum Ratio (MR) and (regularized) Zero Forcing (ZF) precoders are implemented. The symbols are oversampled with a factor 4 in the time domain. Following amplification, possibly inducing nonlinear distortion, the signals are transmitted via the channels and further considered both at the locations of the intended users and observer points in the coverage area. In the following, we discuss the channels generated by means of the RTS software and the implemented nonlinear PA model. Furthermore, we show what evaluation metrics are available in the framework to analyze a given scenario.

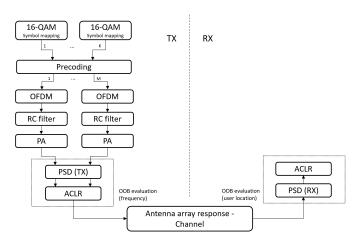


Fig. 1. Overview of the simulation framework.

# A. Channel generation and PA modeling

Channel models are realized based on RTS software, implementing highly realistic and practical models based on the channel models developed in the METIS project [9]. A particular strength of the simulator is that it is able to trace a large number of rays. It is able to capture absorption and reflection phenomena, and generates detailed channel responses including reflections, diffraction and diffuse scattering phenomena. Any area, of particular interest being dense urban surroundings, can be selected via Open Street Map<sup>1</sup> and added to the framework. The height of buildings can be altered

<sup>1</sup>www.openstreetmap.org is an open license map of the world. The selected area can be added by means of its coordinates.

in the extracted data, if necessary. Antennas and arrays of selected size can be implemented by feeding their pattern to the simulator. The number of antennas at the BS is hereby denoted as M. The antennas can be placed on a location of preference. Users can be assigned a specific antenna and location as well. The number of User Equipments (UEs) is denoted as K. One of the outputs of this simulator are the realistic massive MIMO channel responses with dimension  $[M \times K \times f]$  with f for frequency. Note that OOB frequencies are considered as well. We are investigating the 3.5 GHz band, which is currently worldwide the most appropriate for TDD-based massive MIMO, with a bandwidth B equal to 40 MHz. The nonlinear behavior of the PA is modeled with a third-order nonlinear term in function of the input signal s:

$$s_{pa} = s_{norm} - \alpha \cdot s_{norm}^3,\tag{1}$$

where  $\alpha = 1 - 10^{-1/20}$ . The normalization factor  $s_{norm}$  is calculated as:

$$s_{norm} = \frac{s}{\sigma_s \cdot 10^{\text{BO}/20}},\tag{2}$$

with  $\sigma_s$  the standard deviation of input signal *s*, in other words the power of the signal. The input power back-off (BO) of the amplifier, expressed in dB, is an input parameter of this PA model. So, in our model we can specify how far from the saturation point we want the PA to operate and thus manipulate the level of nonlinearity caused by the PA.

#### B. Performance evaluation metrics

The following Key Performance Indicators (KPIs) are defined and implemented in our simulation framework, to be able to objectively analyze different scenarios. We calculate the Power Spectral Density (PSD) in Python with Welch's method [10]. It is expressed in dB/Hz and calculated for IB as well as OOB frequencies. Based on [11], we calculate the Adjacent Channel Leakage Power Ratio (ACLR) in a MIMO environment as follows:

$$ACLR \triangleq \frac{\max\left\{\int_{-3B/2}^{-B/2} \operatorname{PSD}(f) \mathrm{d}f, \int_{B/2}^{3B/2} \operatorname{PSD}(f) \mathrm{d}f\right\}}{\int_{-B/2}^{B/2} \operatorname{PSD}(f) \mathrm{d}f},$$
(3)

which is expressed in dB. The numerator selects the maximum of respectively the left and right adjacent frequency band, both with bandwidth *B*. A graphical result is available in the OOB heatmap where the OOB power in dB is indicated by a colored scale on top of the geographical area (as in the example given in Fig. 2). An important contribution of this spatial evaluation of the OOB power is the ability to detect IM beams. These out-of-band beams can occur when multiple signals are fed to a nonlinear component, and in general are beamed towards more (different) directions than the in-band signals [8].

To evaluate the IB signal quality, the Error Vector Magnitude (EVM) is calculated as follows:

$$EVM \triangleq \frac{\left\| (\mathbf{QAM}_{\mathrm{TX}} - \mathbf{QAM}_{\mathrm{RX}})^2 \right\|}{\left\| \mathbf{QAM}_{\mathrm{TX}}^2 \right\|},\tag{4}$$

with  $QAM_{TX}$  the transmitted QAM symbols and  $QAM_{RX}$  the received QAM symbols.  $\|.\|$  is the absolute value operator for complex signals. Another IB quality evaluation can be performed by means of the constellation diagram of the received QAM symbols. This visualization clearly indicates whether or not the received symbols are interpretable after transmission. Similar to the OOB heatmap, an IB heatmap is possible as well. These IB metrics are applied for verification of the framework, it is not explicitly used in the analysis below.

### C. Grid of observers and users

We divide the considered coverage in grid points, where each grid point is either an observer point or an intended user, allowing us to assess both IB performance and OOB emissions at locations where users in adjacent may want to communicate. We thus sample the received power over a predefined area. The granularity of the grid is limited by computation resources. We have divided the area in 625 grid points, or 25 x 25, for example visible in Fig. 2.

#### **III. SYSTEM PARAMETERS AND SCENARIO VALIDATION**

To analyze this multi variable and thus complex matter, we constraint some parameters and circumstances. We also describe in this section how we validated the framework with a scenario where the IM beams are predictable.

# A. General scenario parameters

We here allocate some parameters and circumstances of the scenarios considered in the further analysis and presented results. The following parameters apply, unless specified otherwise:

- The BS is equipped with 128 patch antennas in a Uniform Linear Array (ULA) topology and is positioned at the center of the left edge of the considered area.
- The antenna spacing at the BS is  $0.5\lambda$  with  $\lambda$  the wavelength of the center frequency of 3.5 GHz.
- The BS is standard located at a height of 29 m. Exception to 50 m is made in view of creating LoS conditions.
- The UEs are equipped with a single isotropic antenna, located at a height of 1.5 m.
- The map area is the KU Leuven Technology Campus in Ghent<sup>2</sup>, size 440 m x 444 m. The site includes relatively high buildings as well as some open space and is a good representation of an urban environment.
- The PA BO is 7 dB.
- Precoding is realized with MR.

# B. LoS and nLoS scenarios

The scenarios in an urban environment inherently contain multipath components because of scattering, reflection, diffraction, etc. We expect these *NLoS scenarios* to be favorable for distributing OOB emission spatially. To create a pure *LoS scenario* of which we expect it to follow theoretical predictions, we put both the BS and the UEs at an elevated height of 50 m. With that height, we are certain that no

<sup>2</sup>https://iiw.kuleuven.be/english/ghent/contact

building will interfere or block the signal. It should be noted that an accidental LoS beam between a UE and the BS could occur in a NLoS scenario. However, we look at the bigger picture of the complete area.

# C. Framework validation on predicted scenario

To validate the correctness of the results of the simulation framework, a scenario with theoretically predictable outcome is simulated. We assume a bandlimited system such that only  $2f_1 - f_2$  and  $2f_2 - f_1$  frequencies will be radiated in the neighbouring band. The simple case of two users in a LoS is considered, where the angle towards the BS is denoted as  $\theta_i$ . The boresight of the antenna array, perpendicular on the array, is the reference angle of 0°. The angles of the IM beams  $\theta_{IM,A}$  and  $\theta_{IM,B}$  can be calculated as:

$$\theta_{IM,A} = \sin^{-1} \left( \frac{2f_1 \cdot \sin \theta_1 - f_2 \cdot \sin \theta_2}{2f_1 - f_2} \right)$$
(5)

$$\theta_{IM,B} = \sin^{-1} \left( \frac{2f_2 \cdot \sin \theta_2 - f_1 \cdot \sin \theta_1}{2f_2 - f_1} \right).$$
(6)

Assuming for an approximate estimate of these angles that  $f_1 \approx f_2$ , these formulas simplify to:

$$\theta_{IM,A} \approx \sin^{-1} \left( 2\sin\theta_1 - \sin\theta_2 \right) \tag{7}$$

$$\theta_{IM,B} \approx \sin^{-1} \left( 2\sin\theta_2 - \sin\theta_1 \right) \tag{8}$$

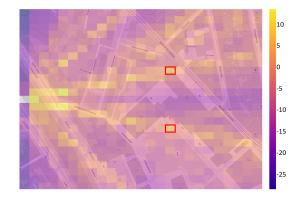


Fig. 2. OOB heatmap of a LoS experiment with two users on  $15^{\circ}$  and  $-15^{\circ}$ , indicated by the red squares, with BS at the center of the left edge.

The experiment is carried out with  $\theta_1 = -\theta_2 = 15^\circ$ , which should yield in intermodulation beams in the directions  $\theta_{IM,A} = -\theta_{IM,B} \approx 50,94^\circ$ . Fig. 2 is the OOB heatmap of this scenario with the BS ULA antenna array centered on the left side of the area. We clearly distinguish two beams to the users at  $\theta_1$  and  $\theta_2$ , and two IM beams at about  $50^\circ$  and  $-50^\circ$ . This experiment validates the simulation framework with an outcome that was theoretically predicted.

## **IV. RESULTS**

In Section III-C, we investigated a specific predictable scenario under LoS conditions, as described in Section III-B. We here extend the analysis for handpicked scenarios that we anticipate to be representative for diverse cases of special interest. The first case (not shown in view of space constraints) is a single user LoS scenario, where the simulations confirm the theoretically predicted results that no intermodulation beams are generated, and the OOB emissions receive array gain similar to the IB signals. A next interesting case, is the NLoS version of the scenario in Section III-C, for which the resulting OOB heatmap is shown in Fig. 3. A completely different spatial distribution pattern of the OOB is observed. It is important to notice that the color scale has shifted down, meaning that the intensity of OOB emissions has decreased, as also theoretically predicted for multi-path conditions. Still, the observed OOB shows high variations with up to 20 dB over different locations.

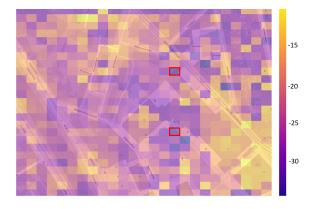


Fig. 3. OOB heatmap of a NLoS experiment with two users with  $\theta_1 = 15^{\circ}$  and  $\theta_2 = -15^{\circ}$ , indicated by the red squares, with BS at the center of the left edge.

We conduct a similar LoS and NLoS experiment, now with  $\theta_1 = 80^\circ$  and  $\theta_2 = 29.5^\circ$ . Then, we expect an IM beam in the 'favorite' direction of the antenna array, namely at  $0^\circ$ . The result confirms this as demonstrated in Fig 4. In case highly directive antenna elements are used, this could lead to significant OOB emissions in this direction with respect to power transmitted in the directions of the intended users.



Fig. 4. OOB heatmap of a LoS experiment with two users with  $\theta_1 = 80^{\circ}$  and  $\theta_2 = 29.5^{\circ}$ , indicated by the red squares, with BS at the center of the left edge.

The corresponding experiment in NLoS conditions yields a much more scattered result, as seen in Fig. 5. These NLoS results confirm that more multi-path components lower coherent combining of OOB components from the many antennas in massive MIMO transmission. Still, the spatial distribution of the OOB emissions is far from uniformly distributed as theoretically predicted for i.i.d. Rayleigh fading channels. We have also assessed NLoS scenarios with more than 10 users randomly distributed over the considered area, providing very similar results.



Fig. 5. OOB heatmap of a NLoS experiment with two users with  $\theta_1 = 80^{\circ}$  and  $\theta_2 = 29.5^{\circ}$ , indicated by the red squares, with BS at the center of the left edge.

A last investigated scenario compares MR and ZF precoding with two users on the same LoS when seen from the BS. It is known that MR precoding will result, in this setting, in a bad EVM due to considerable multi-user interference distortion, while the ZF can still achieve good user separation. The results of the OOB analysis, depicted in Fig. 6, demonstrate that the ZF is also better from this perspective, as it clearly spreads the distortion more uniformly in space. It should be noted that in practical deployments a regularised ZF precoding is preferred.

## V. DISCUSSION OF RESULTS IN A REGULATORY CONTEXT

In the context of OOB emissions, the legacy ACLR regulations are the so-called *conducted measurements*. In that case, the ACLR measured at the Antenna Reference Point (ARP) must be below a predefined threshold. The biggest question here is what this ARP should be in the case of massive MIMO. There is the consensus that we should not be looking at each antenna element separately but all of them combined, thus the antenna array rather than its elements. However, as [7] states, this type of measuring ignores the Array Gain (AG) and the

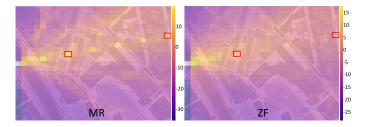


Fig. 6. OOB heatmap for MR vs ZF precoding for a situation with two users on the same LoS.

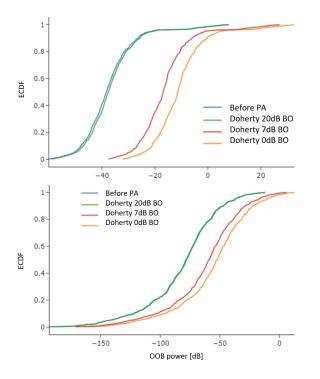


Fig. 7. ECDF of LoS single user (upper) and NLoS 4 user case (lower). Notice the different x axes because of the large spread of OOB power and the overlap of the green and blue curve in the figure at the bottom.

effect it could have on the OOB radiation. A second type of measurements are the so-called *over-the-air measurements*, where the measurements are done at selected positions around the BS. Our OOB heatmaps offer a clear visualization of this second type of measurement. The results demonstrate that OOB is far from uniformly distributed in space. One may argue that conducting measurements *everywhere* and for *numerous user combinations* is required to guarantee that regulations are violated *nowhere and never*. The theoretical analysis and simulation-based assessment can help to predict and provoke worst case OOB scenarios, as we have done in our study.

Moreover, one may also question the sustainability of current regulations. Indeed, setting the back-off of the PAs at a level such that regulations will nowhere and never be violated may result in a low efficiency, while compliance is reached in most places also when working closer to saturation at higher efficiency. To this end, we depict Empirical Cumulative Distribution Function (ECDF) curves in Fig. 7 for the OOB power measured at all observer locations for the two distinct cases: a situation with a single user in LoS on the one hand, and four users in NLoS on the other hand. First of all, it shows the large variations in space. Also, the considerable different ECDF for different user scenarios suggest that in scenarios that may require a relative high output power to achieve good inband performance (multiple users, NLoS), one may afford to operate the PAs closer to saturation in a more efficient regime.

# VI. CONCLUSIONS AND FUTURE WORK

We investigated OOB distortion in a massive MIMO environment under realistic conditions by means of a simulation framework with integrated RTS channels. The performance evaluation metrics allow us to objectively analyze different scenarios. The framework was verified by fact-checking the simple scenario of two users in a LoS environment with predictable IM beams.

We can conclude that the spatial distribution of OOB in realistic scenarios is not well predicted by theoretical analysis where specific simplified channel models are applied. Despite multi-path environments and multi-user scenarios, the results don't show uniformly distributed OOB. This reveals that the assumption of non-correlated distortions terms is also in these cases over-simplifying. The environment itself might not resolve the OOB violations. Significant beamforming gain in the OOB radiation is observed in LoS as well as NLoS scenarios. Our experience is that the RTS software is able to capture the complexity of the matter.

We comment that conventional regulations need revision for massive MIMO environments. The evident next step is to find solutions to the problematic situations where OOB distortions exceed the regulations. These could involve dedicated user scheduling and adequate precoding approaches.

#### ACKNOWLEDGMENT

We would like to thank NVIDIA for providing the GPU that greatly accelerated our simulations.

#### REFERENCES

- S. R. Danve, M. S. Nagmode, and S. B. Deosarkar, "Energy Efficient Cellular Network Base Station: A Survey," in 2019 IEEE Pune Section International Conference (PuneCon), 2019, pp. 1–4.
- [2] E. Björnson, J. Hoydis, M. Kountouris, and M. Debbah, "Massive MIMO Systems With Non-Ideal Hardware: Energy Efficiency, Estimation, and Capacity Limits," *IEEE Transactions on Information Theory*, vol. 60, no. 11, pp. 7112–7139, 2014.
- [3] C. Desset and L. Van der Perre, "Validation of low-accuracy quantization in massive MIMO and constellation EVM analysis," in 2015 European Conference on Networks and Communications, 2015, pp. 21–25.
- [4] S. P. Yadav and S. C. Bera, "Nonlinearity effect of high power amplifiers in communication systems," in 2014 International Conference on Advances in Communication and Computing Technologies (ICACACT 2014), 2014, pp. 1–6.
- [5] I. T. U. (ITU), "Unwanted emissions in the out-of-band domain," https://www.itu.int/dms\_pubrec/itu-r/rec/sm/R-REC-SM. 1541-6-201508-I!!PDF-E.pdf, 2015, accessed: 2021-04-28.
- [6] E. G. Larsson and L. Van der Perre, "Out-of-Band Radiation From Antenna Arrays Clarified," *IEEE Wireless Communications Letters*, vol. 7, no. 4, pp. 610–613, 2018.
- [7] C. Mollén, E. G. Larsson, U. Gustavsson, T. Eriksson, and R. W. Heath, "Out-of-Band Radiation from Large Antenna Arrays," *IEEE Communications Magazine*, vol. 56, no. 4, pp. 196–203, 2018.
- [8] R. J. Mailloux, *Phased Array Antenna Handbook*, 3rd ed. USA: Artech House, Inc., 2017.
- [9] J. Medbo, K. Börner, K. Haneda, V. Hovinen, T. Imai, J. Järvelainen, T. Jämsä, A. Karttunen, K. Kusume, J. Kyröläinen, P. Kyösti, J. Meinilä, V. Nurmela, L. Raschkowski, A. Roivainen, and J. Ylitalo, "Channel modelling for the fifth generation mobile communications," in *The 8th European Conference on Antennas and Propagation (EuCAP 2014)*, 2014, pp. 219–223.
- [10] P. Welch, "The use of fast Fourier transform for the estimation of power spectra: A method based on time averaging over short, modified periodograms," *IEEE Transactions on Audio and Electroacoustics*, vol. 15, no. 2, pp. 70–73, 1967.

[11] C. Mollén, U. Gustavsson, T. Eriksson, and E. G. Larsson, "Out-of-band radiation measure for MIMO arrays with beamformed transmission," in 2016 IEEE International Conference on Communications (ICC), 2016, pp. 1–6.